Structure and solvation forces in confined films: Linear and branched alkanes

Jianping Gao, W. D. Luedtke, and Uzi Landman
School of Physics, Georgia Institute of Technology, Atlanta, Georgia 30332

(Received 1 November 1996; accepted 4 December 1996)

Equilibrium structures, solvation forces, and conformational dynamics of thin confined films of *n*-hexadecane and squalane are investigated using a new grand canonical ensemble molecular dynamics method for simulations of confined liquids. The method combines constant pressure simulations with a computational cell containing solid surfaces and both bulk and confined liquid regions in equilibrium with each other. For both molecular liquids layered density oscillations in the confined films are found for various widths of the confining gap. The solvation force oscillations as a function of the gap width for the straight chain *n*-hexadecane liquid are more pronounced exhibiting attractive and repulsive regions, while for the branched alkane the solvation forces are mostly repulsive, with the development of shallow local attractive regions for small values of the gap width. Furthermore, the nature of the transitions between well-formed layered configurations is different in the two systems, with the *n*-hexadecane film exhibiting solid-like characteristics portrayed by step-like variations in the number of confined segments occurring in response to a small decrease in the gap width, starting from well-layered states of the film. On the other hand the behavior of the squalane film is liquid-like, exhibiting a monotonic continuous decrease in the number of confined segments as the gap width is decreased. These characteristics are correlated with structural properties of the confined films which, for *n*-hexadecane, exhibit enhanced layered ordering and in-plane ordered molecular arrangements, as well as with the relatively high tendency for interlayer molecular interdigitation in the squalane films. Reduced conformational (*trans-guache*) transition rates in the confined films, compared to their bulk values, are found, and their oscillatory dependence on the degree of confinement is analyzed, showing smaller transition rates for the well-formed layered states of the films. © *1997 American Institute of Physics.* [S0021-9606(97)50610-6]

I. INTRODUCTION

Understanding the structure, dynamics, and rheology of ultrathin films (of nanometer scale thickness) of low molecular weight hydrocarbons adsorbed on solid surfaces, and in particular of such films confined between solids, is of fundamental interest as well as practical importance for many processes, such as lubrication, adhesion, coatings, chromatography, and membrane separation. Indeed, the properties of such systems have been the subject of numerous investigations (for recent reviews, see Refs. 1–5) employing sensitive microscopies [the surface force apparatus (SFA), atomic force microscopy (AFM), and friction force microscopy (FFM)], computer simulations,[1,6–9] and other theoretical approaches.[10–15]

Focusing here on confined films, certain key features pertinent to our current study, extracted from a large body of available literature on the subject, may be summarized as follows:

(i) Liquids confined between solid boundaries (as well as those adsorbed on a solid surface) tend to organize into layered structures,[1,10,11] that is strata parallel to the solid surfaces, provided that the boundary is smooth compared to the molecular scale. In such structures the mean local density of the liquid oscillates with distance normal to the boundary, and this underlies oscillations in the force between the confining boundaries as the distance between them (i.e., the confining gap width) is varied, with a period approximately equal to the molecular width.

(ii) Such oscillatory solvation forces between confining surfaces[11] were observed and calculated for simple liquids[16] (e.g., modeled as spheres), nonpolar globular molecules[17–19] (e.g., octamethylcyclotetrasiloxane, OMCTS), straight chain alkanes[6,20–25] (e.g., *n*-hexadecane, n-$C_{16}H_{34}$), and even for chain molecules with a single pendant methyl group,[18] such as 3-methylundecane, $C_{12}H_{26}$, (although in earlier measurements[26,27] of force-distance profiles of 2-methyloctadecane and 2-methylundecane vanishing of the oscillations and the observation of a single attractive minimum have been reported, the possibility of lack of equilibration in these measurements was subsequently raised).[11,29] On the other hand solvation force measurements[18,29] for a longer and more heavily branched molecule (i.e., 2,6,10,15,19,23-hexamethyltetracosane, or squalane, a molecule with a C_{24} backbone and six, symmetrically placed, methyl side groups) confined between mica surfaces have revealed disappearance of the force oscillations, with a

Downloaded¬04¬Feb¬2004¬to¬130.207.165.29.¬Redistribution¬subject¬to¬AIP¬license¬or¬copyright,¬see¬http://jcp.aip.org/jcp/copyright.jsp

sole broad attractive minimum at a gap width $D=18$ Å, and what appears as a hard wall repulsion at $D=16$ Å (measurements for smaller gap width have not been attempted).[18] From these observations it has been concluded that branching (via pendant methyl groups) can disrupt oscillatory forces, though the degree of branching must be moderately large.[18]

(iii) Confined ultrathin films[30] may exhibit two different responses (in shear,[30] as well as in response to variation of the normal distance between the confining surfaces);[19] a liquid-like response in which the liquid responds to the deformation by flow,[30] or spreading (as in drainage measurements),[31,32] and a solid-like response characterized by observation of the development of ''yield stress'' in the confined fluid,[33] portrayed by lack of deformation over macroscopic distances unless a critical shear stress is attained (leading to the development of ''stick'' and ''slip'' patterns).[33–36] Additionally, recent SFA measurements[19] on confined films of OMCTS (whose diameter is $\sim$ 9 Å), suggest the abrupt development of solid-like behavior in relatively thick films of 6 layers. It should be emphasized that in these measurements the transition from liquid-like behavior for a 7-layer film to a solid-like one for a 6-layer film has been induced solely by the additional confinement (i.e., without an imposed lateral motion of the confining surfaces). In this context we remark that liquid layering and force oscillations have also been predicted recently[37] in molecular dynamics simulations of *n*-hexadecane films sheared between solid surfaces containing structural nonuniformities (asperities). In these studies the density oscillations occurred in the liquid region between the approaching asperities leading to oscillatory variations in the lateral force. Furthermore, a transition from liquid-like response at large interasperity distances to a soft solid-like one when the two asperities approach each other, has been described and analyzed using a rheological nonlinear Maxwell model, extending elastohydrodynamics to the nanoscale regime.[7,37]

(iv) Liquid dynamics at interfaces and particularly under confinement is influenced in a marked way, becoming more ''sluggish'' in nature with increased confinement of the fluid.[30] Furthermore, molecular architecture and complexity appear to influence the dynamics of confined liquids. Thus, for example, in a homologous series of confined polymers, long chain molecules are found to be more sluggish than shorter chains.[38] These effects on the molecular dynamics of interfacial and confined complex liquids pertain both to intra and intermolecular relaxation times, and depend also on the strength of interactions between the confined molecules and the solid surfaces.[21,24]

On the theoretical front interfacial and confined liquids have been investigated using both analytical methods[10] and computer-based simulations.[1,6–9,16,22–25,28,35–37] In particular molecular dynamics (MD) and Monte Carlo (MC) simulations allow direct investigation of such complex systems with atomic-scale spatial and temporal (using MD) resolution. While early simulations employed model monoatomic simple liquids interacting via central-force pairwise additive potentials (i.e., Lennard-Jones interatomic potentials), more recent ones (see reviews in Refs. 1,5–8) focus on liquids of a more complex molecular structure (e.g., alkanes) with various degrees of complexity (and realism) of the inter and intramolecular interactions. Such simulations have revealed a wealth of information pertaining to energetic, structural, dynamical, and rheological properties of interfacial and confined molecular liquids under static and shear conditions. In these simulations the confining surfaces were modeled as structureless boundaries or as atomically structured solid surfaces, and for various configurations. In most simulations the confining surfaces and the confined liquids were extended indefinitely, or alternatively the liquid has been modeled as a confined droplet[28] (or semidroplet).[21] Extensive simulations have also been performed for complex liquids adsorbed on atomically structured solid surfaces, interacting with tips (modeling AFM and FFM experiments); in this context, see Refs. 6, 22 and 23 for simulations of the interactions between tapered (blunt) tips and adsorbed liquid films using an *ad hoc* grand canonical ensemble,[22(b)] where the layered structure and solvation force oscillations of a confined *n*-hexadecane liquid in AFM and FFM have been predicted, as well as investigations of cavitation phenomena associated with withdrawal of immersed tips.[23]

The configuration of both SFA and tip-based experiments is that of a confined liquid in thermodynamic equilibrium with a surrounding bulk fluid (or unconfined film). Consequently, the measured force (or pressure) is more appropriately described as a disjoining force (or pressure) which is the difference between the force (pressure) in the confinement and that of the bulk fluid with which the confined film is in equilibrium.[10,11] Therefore it is desirable to conduct simulations of such systems under grand canonical (GC) ensemble conditions (i.e., constant chemical potential μ, pressure P, and temperature T). An early formulation of grand canonical ensemble MC simulations[39,40] (GCEMC, where $\mu, T,$ and the volume were held constant) has been used in studies of confined simple liquids. In this method fluid molecules are inserted or eliminated from the system according to the grand canonical ensemble distribution function with the value of μ determined separately from bulk fluid simulations.

In this paper we describe a grand canonical (μPT) molecular dynamics (GCMD) method for simulations of confined lubricants of complex molecular structure (in our case, *n*-hexadecane and squalane). The method which we developed combines constant pressure MD with a computational cell containing both bulk and confined fluid regions, allowing systematic GCMD investigations of confined liquids, and alleviating the difficulties associated with insertion of mol-

Downloaded¬04¬Feb¬2004¬to¬130.207.165.29.¬Redistribution¬subject¬to¬AIP¬license¬or¬copyright,¬see¬http://jcp.aip.org/jcp/copyright.jsp

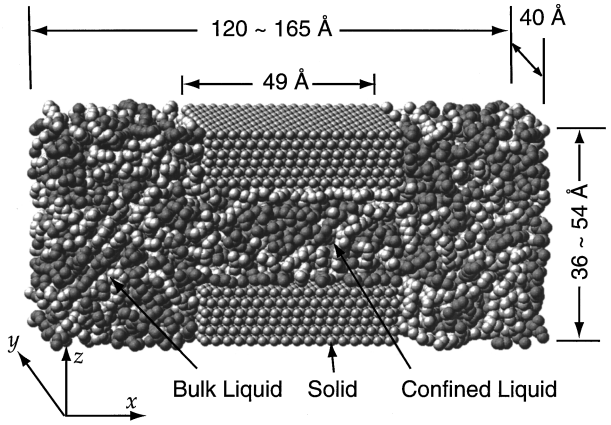

FIG. 1. View of the three-dimensional (3D) computational cell for grand canonical molecular dynamics simulations of confined liquids. The cell is repeated using 3D periodic boundary conditions. It contains solid substrates (small spheres) of finite extent in the x direction and extending through the cell in the y direction. The dimension of the cell in x direction (H_x) varies dynamically in response to the applied external pressure in that direction, taking different values depending on the gap width between the opposing solid surfaces. The cell is filled with liquid molecules, part of them are in the confinement and the rest outside it. H_x is taken to be large enough such that bulk liquid behavior can be established in the regions outside the confinement.

ecules as in the GCEMC method[39,40] which at the densities of interest to us and for the complex molecules which we use would pose significant practical difficulties.

In Sec. II, we describe the formulation and implementation of our GCMD method. Results of comparative simulations of confined n-hexadecane and squalane films are presented in Sec. III, followed by a summary given in Sec. IV.

II. GRAND CANONICAL MD FOR CONFINED LIQUIDS

In this section we describe the formulation and implementation of a grand canonical molecular dynamics (GCMD) method for simulations of confined liquid systems and discuss pertinent details of our simulations. An overview of the simulated system is shown in Fig. 1. The simulation cell contains both liquid (alkane) molecules and solid blocks, with periodic boundary conditions extending the system in all three directions. The solid blocks are of finite size in the x and z directions, with the distance between the two solid surfaces in the z direction defining the width of the gap (D) confining the fluid (in our simulations the solid surfaces forming the gap in the middle of the cell are modeled as gold (111) planes). In the y direction, the solid blocks are extended through the whole cell. The rest of the space in this 3-dimensional cell is filled with alkane molecules; in this paper, we have studied two different alkane liquids: linear n-hexadecane ($n-C_{16}H_{34}$) and a branched alkane, i.e., squalane ($C_{30}H_{62}$).

To facilitate studies of the properties of the confined alkane thin films, which are in equilibrium with a surrounding bulk liquid, the solid blocks as shown in Fig. 1 are arranged to create two regions of the alkane fluid. Inside the gap, between the two solid surfaces, the alkanes are confined as a thin film with a thickness D ranging between 10 and 30 Å. The size of the cell in the x direction is taken to be sufficiently large so that the alkanes in the regions outside the confined one can exhibit bulk liquid alkane behavior. The size of the computational cell in the z direction is varied to give the desired film thickness in the gap. In our simulations the extent of the solid blocks in the x direction is 49 Å and the height of each block is $d_s=13$ Å; the size of the cell in the z direction H_z is thus given by $H_z=2d_s+D$, and the size of the cell in the y direction is kept constant, $H_y=40$ Å. The size of the cell in the x direction H_x is allowed to vary dynamically, using constant pressure MD,[41] from $\sim$ 120 Å to $\sim$ 165 Å, depending on the gap width D. The hydrostatic pressure, determining the magnitude of H_x, is taken to be one atmosphere; on the scale of all other stresses in the system this represents a vanishingly low pressure.

In this study, the alkane molecules are treated dynamically while the gold atoms of the solid substrates are static (treating the solids dynamically does not affect our results); the solid gold blocks contain a total of 3520 atoms which are immersed in 206 to 234 squalane or 242 to 400 n-hexadecane molecules (for sufficiently thin films bulk behavior in the regions outside the confinement can be achieved for a smaller number of molecules in the computational cell). The equations of motion of the alkane segments are solved by the Verlet algorithm with an integration time step of 3 femtoseconds. The temperature of the system is controlled via scaling of the atomic velocities at infrequent intervals (when equilibrium is reached no temperature control is necessary); the temperature for these simulations is 350 K which allows the systems to equilibrate in a reasonable amount of computing time.

The alkane molecules are represented by the united atom model, without rigid constraints. The intramolecular potentials include bond stretching, bond angle bending, torsional angle, and Lennard-Jones (LJ) interactions between all atom pairs separated by more than three bonds. The bond stretching is represented by a stiff linear spring, with the bond force constant reduced by a factor of 4 from its realistic value to facilitate computations with an increased time step (this has no effect on our results). The angle bending, torsional potentials, and LJ potentials describing intra- and inter-alkane interactions are the same as those used by Mondello and Grest[42] in their recent study of n-alkanes and squalane. A LJ potential is used to describe the interactions between the alkane segments and the gold atoms of the solid substrates, with parameters fitted to experimental desorption data, as described by us previously.[21,43]

The initial configuration of the system is set up with a large value of the gap width ($\sim$ 28 Å). A random walk with fixed bond lengths and bond angles is employed to place the alkane molecules into the computational cell. The nonbonded interactions are not considered during the random walk, but the molecular segments are not allowed to be too close to the solid blocks. After all molecules have been placed into the computational cell, a molecular dynamics simulation with an upper-bound set on the nonbonded forces is carried out to eliminate segmental overlaps which may

Downloaded¬04¬Feb¬2004¬to¬130.207.165.29.¬Redistribution¬subject¬to¬AIP¬license¬or¬copyright,¬see¬http://jcp.aip.org/jcp/copyright.jsp

have been generated in the initial random walk stage; in this procedure, the maximum LJ force allowed between a pair of interacting segments is limited to $f_{LJ}(r=0.85\sigma)$, where σ is the LJ length parameters. We have found this procedure to be very effective in generating initial configurations of alkane liquids. Subsequently, the upper limit on the force is removed and a MD run of several hundred picoseconds is performed to allow the system to fully equilibrate.

For a given value of alkane film thickness D, which is the distance between the two solid surfaces confining the alkanes, the squalane systems are equilibrated for 300–1000 ps followed by a simulation period of 120–300 ps, during which the computed properties are time averaged; for the *n*-hexadecane systems, the equilibration periods are usually 60–480 ps and the data acquisition periods are typically 120 ps (the longer equilibrium periods were used for the thinner films). The time histories of several energetic and structural properties were monitored to assure that equilibration has been achieved after each adjustment of the gap width; such adjustments involve squeezing of the film to the next gap width through a slow decrease of D, followed by a prolonged equilibration period at the required gap width as described above. During the squeezing process and the first part of the equilibration, the number of molecules in the confined region decreases as some molecules are pushed into the bulk region where the pressure remains constant via dynamical variation of H_x. For the squalane film, reversal of the process at several values of the gap width (i.e., decreasing the confinement) resulted in only slight hysteresis in calculated properties (e.g., solvation force), confirming adequate equilibration.

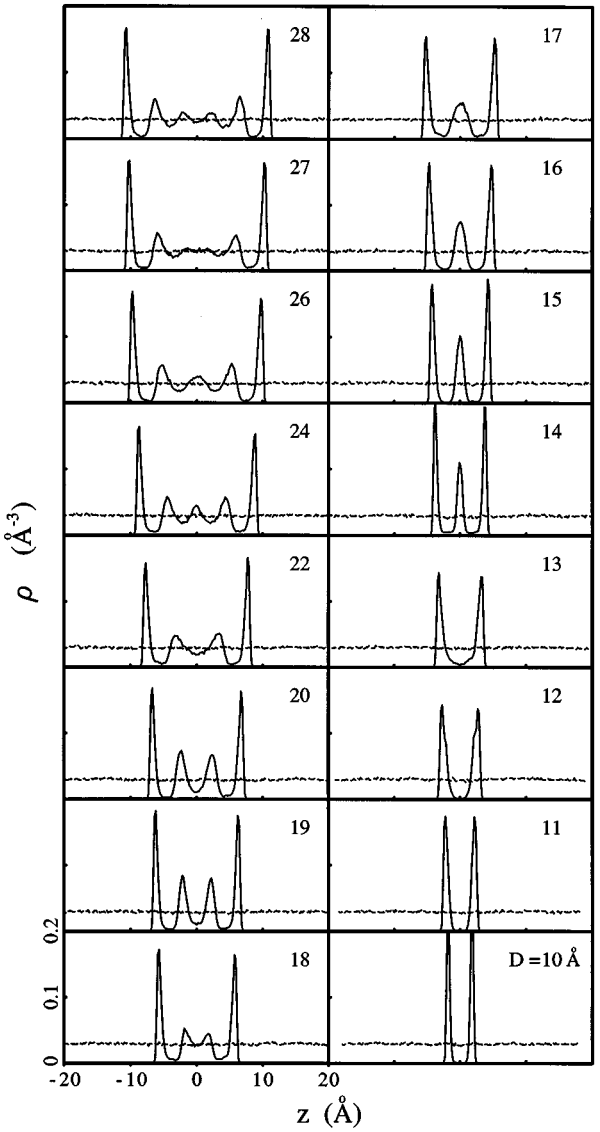

FIG. 2. Equilibrium segmental density profiles for *n*-hexadecane along the *z* direction (normal to the confining solid surfaces); solid lines correspond to the film in the confined region and the dashed lines calculated for the region outside the gap. The gap widths (D) for which the profiles were calculated are indicated. The well-formed layered configurations [see maxima in the solvation force curve in Fig. 5(a)] correspond to $D=10$, 14, 19, and 24 Å. The other equilibrium profiles were calculated for intermediate values of D. Note that the liquid density outside the confinement (dashed line) is uniform and remains constant for all values of D, while the layered density features in the confined film (particularly in the middle region of the film) vary in sharpness depending on the degree of confinement, becoming the sharpest for the values of D corresponding to well-formed layers. Distances in unit of angstroms.

III. RESULTS

Using the new simulation method described in Sec. II we have investigated the structures and properties of interfacial *n*-hexadecane (n-$C_{16}H_{32}$) and squalane (2,6,10,15,19,23-hexamethyl-tetracosane) films confined between two opposing surfaces modeled to represent Au(111) surfaces. As described in Sec. II the confined films are in equilibrium with the surrounding liquid in which the confining solids are immersed.

A. Layering transitions and solvation forces

We begin by presenting our results for the segmental density profiles $\rho(z)$ for the two systems, recorded versus distance in the direction normal to the surfaces, for a sequence of separations (gaps) between the confining surfaces. Such profiles are shown for *n*-hexadecane in Fig. 2 and for squalane in Fig. 3. The solvation forces (i.e., the total force exerted by the interfacial film on the confining surfaces, which is the same as the force which would be required in order to hold the two surfaces at the corresponding separation) recorded for the two systems during the approach of the two surfaces, are shown for *n*-hexadecane and squalane in Fig. 4. Additionally, we display in Fig. 5 records of the number of molecular segments confined in the gap between the two surfaces, n_{cfn}, as a function of the width of the gap, D, as well as of n_{cfn}/D plotted versus D.

While the density profiles (Figs. 2 and 3) for both materials exhibit oscillatory patterns, a closer inspection reveals differences between the two cases. Already for large separations between the surfaces (a wide gap, $D=28$ Å) the *n*-hexadecane film appears to be well layered throughout with 6 well-formed layers (Fig. 2, top left), while for the

Downloaded¬04¬Feb¬2004¬to¬130.207.165.29.¬Redistribution¬subject¬to¬AIP¬license¬or¬copyright,¬see¬http://jcp.aip.org/jcp/copyright.jsp

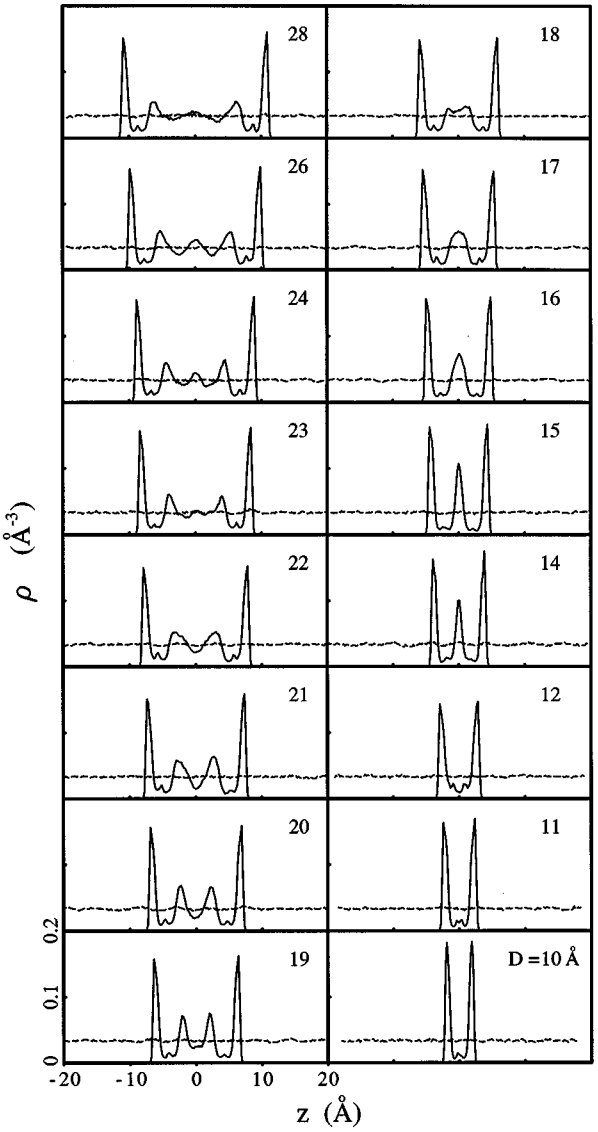

FIG. 3. Same as Fig. 2, but for squalane. The well-formed layer configurations correspond to the maxima in the solvation force shown in Fig. 5(b). Note that small local density maxima on each side of the confined film, located between the interfacial layer and the next layer in; such local maximum between the interfacial layers is seen even for the 2-layer film configurations. The local density minima between layers are not as deep as those found for the *n*-hexadecane film (compare to corresponding configurations in Fig. 2). Distances in units of angstroms.

same gap width the squalane film exhibits only 4 well-formed layers and in the middle region of the gap the density is close to that in the bulk (Fig. 3, top left). We also note for the squalane case the appearance of distinct features between the first interfacial layer on each side of the film and the second layer in, which are absent in the *n*-hexadecane profile. These features, which may also be seen (though less pronounced) between the second and third layer of the squalane film are caused by the methyl branches which lie preferentially between the layers (a similar behavior has been observed in previous simulations of a single-branched hexadecane film).[28]

Decreasing the width of the gap is accompanied by reduction of the number of layers in the film (see Figs. 2 and 3 for $D=24$ Å, where 5 well formed layers are observed for both films). We also remark that the density minima between the layers are deeper for hexadecane. Moreover, for hexadecane these density minima are always below the bulk density, while for squalane they may become larger than that of the bulk liquid density (see e.g., Fig. 3, corresponding to $D=18$ Å).

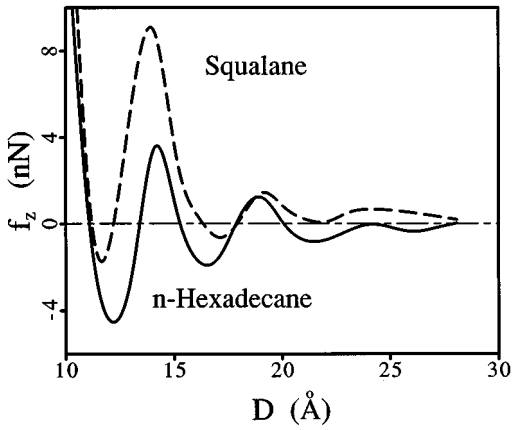

FIG. 4. Equilibrium solvation forces, f_z in *n*N, plotted versus the width of the confining gap, D in Å, calculated for the confined *n*-hexadecane (solid line) and squalane (dashed line) films. Note that for *n*-hexadecane F_z ($D>20$ Å) is negative (attractive) while for the squalane film the force is overall repulsive with small local attractive minima near $D\sim$ 17 Å and $\sim$12 Å. Well-formed layers occur for $D\sim10$ Å ($n_L=2$), 14 Å ($n_L=3$), 19 Å ($n_L=4$), 24 Å ($n_L=5$). The repulsive forces in the squalane film are stronger than in the *n*-hexadecane one.

In both cases narrowing of the gap results in expulsion of molecules from the confined region (''squeezing-out'' of the film) and transition to a film with a smaller number of layers (which remain throughout to be of similar density, i.e., containing approximately the same number of molecular segments), occurring with a periodicity of about 4.5–5 Å. The layering transitions in the confined films are portrayed in solvation force oscillations (Fig. 4). However, while for hexadecane the force oscillates between positive and negative values, with the local positive force maxima corresponding to configurations with well-formed layers, in the squalane case at wider gaps the force does not take negative values, and the amplitudes of the oscillations are smaller than in the hexadecane case. For narrow gaps ($D\lesssim15$ Å) the force maximum associated with a transition from a 3-layer to a 2-layer film is significantly larger in the squalane film than that in the hexadecane one.

Further insights into the layering transition processes are obtained from records of the number of segments in the confined region, n_{cfn}, plotted versus the distance between the confining surfaces (D), shown in Figs. 5(a) and 5(b). In the hexadecane film, for $D\leqslant20$ Å, (i.e., a 4-layer film) n_{cfn} varies in a step-like manner with sharp drops in the number of confined molecules occurring for the transition from a 4-layer film to a 3-layer one, and subsequently from a 3- to a 2-layer film [a weak step-like signature is seen also for the transition from a 5- to a 4-layer film, see Fig. 5(a) for

Downloaded¬04¬Feb¬2004¬to¬130.207.165.29.¬Redistribution¬subject¬to¬AIP¬license¬or¬copyright,¬see¬http://jcp.aip.org/jcp/copyright.jsp

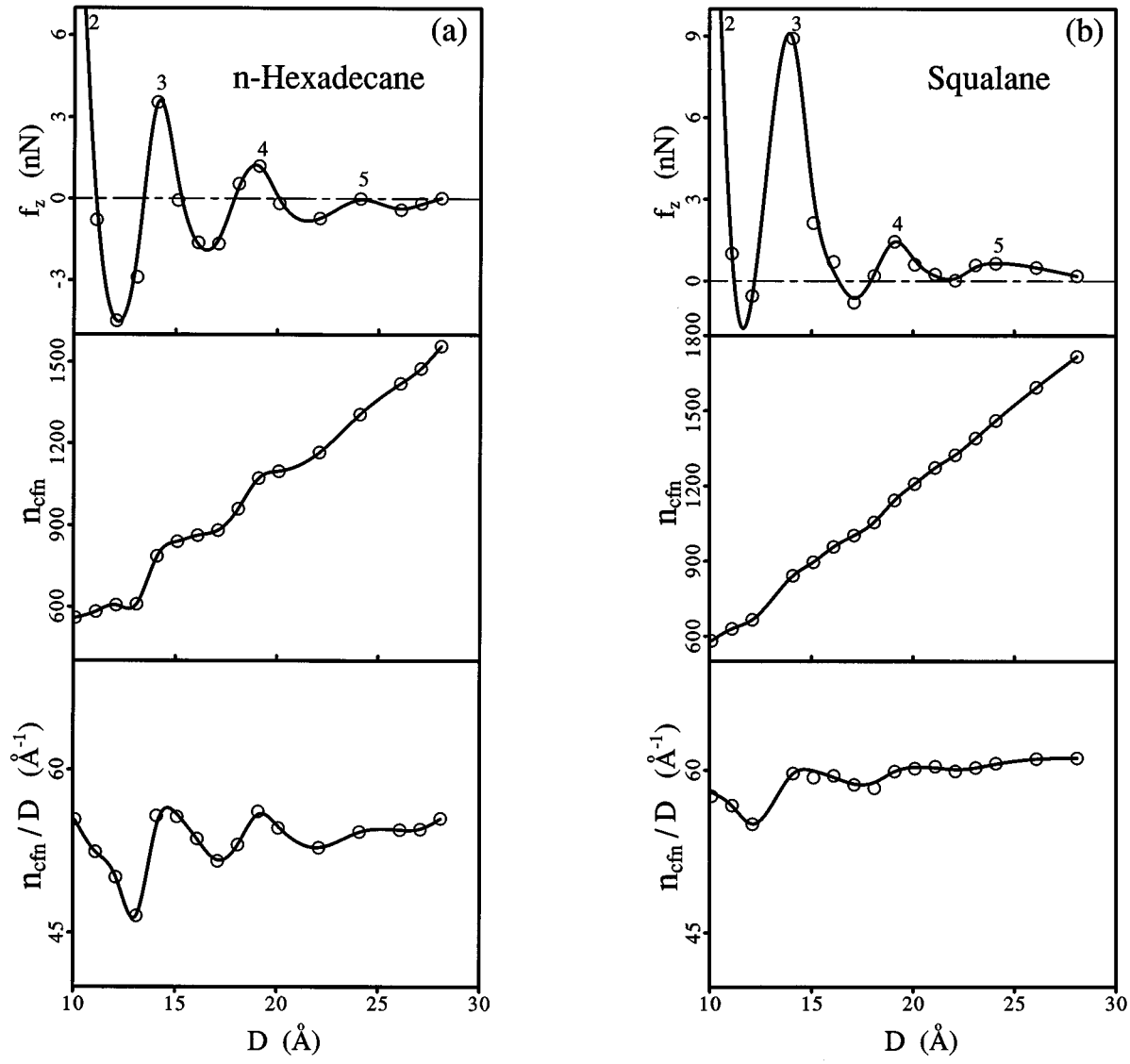

FIG. 5. Solvation force, f_z in nN (upper panel), number of segments in the confining gap, n_{cfn} (middle panel), and n_{cfn}/D (bottom panel), plotted versus the gap width, D, in Å, for the n-hexadecane film (a), and the squalane film (b).

$D \lesssim 25$ Å]. For each of these transitions the drop in n_{cfn} is caused by a relatively small reduction (~ 1 Å) of the gap width from that corresponding to an initial well layered configuration of the film (i.e., the number of layers in the film at the bottom of each step is decreased by one from that corresponding to the film at the top of the step (and the plateau). On the other hand, for the squalane film the variation of n_{cfn} associated with the layering transitions is overall monotonic and continuous in nature, with the development of a weak step-like feature only at the limit of a very thin film [i.e., see transition from a 3- to a 2-layer film, for $D \lesssim 15$ Å, in Fig. 5(b)].

These characteristics of the layering transitions are further found (see Fig. 5) in plots of n_{cfn}/D versus D (where n_{cfn}/D is proportional to the number density of molecular segments in the gap, since the area of the confining solid surfaces is constant for all values of D). These plots illustrate that for the squalane film the confined segmental density remains approximately constant throughout the narrowing (squeezing) process (except in the limit of a very thin film, $D \lesssim 15$ Å), while for n-hexadecane reducing the gap width is accompanied by marked variations in the density (becoming increasingly more pronounced as the film thins down). Furthermore, in the latter case the local maxima of the film density, corresponding to well-formed layered configurations, are of equal value.

These results suggest that the confined squalane film behaves in a liquid-like manner throughout most of the gap-narrowing sequence; that is the equilibrium confined film, which is in contact with the surrounding bulk liquid, maintains a constant density for varying widths of the confining gap by gradually expelling molecules into the surrounding liquid when the gap width is reduced. In contrast the confined n-hexadecane film of sufficiently small thickness (i.e.,

Downloaded¬04¬Feb¬2004¬to¬130.207.165.29.¬Redistribution¬subject¬to¬AIP¬license¬or¬copyright,¬see¬http://jcp.aip.org/jcp/copyright.jsp

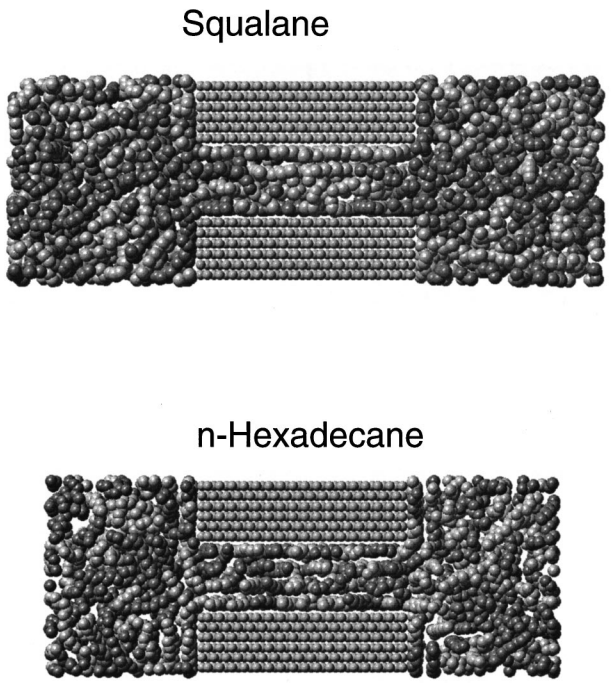

FIG. 6. Side views of the equilibrium 4-layer *n*-hexadecane (bottom) and squalane (top) systems. Note the enhanced order in the *n*-hexadecane confined film. Different shades of molecular segments have been used to aid visualization.

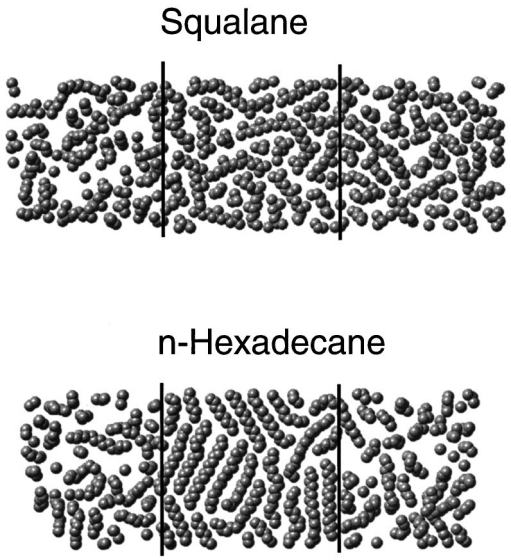

FIG. 7. Top views (in the xy plane) of the interfacial layers of *n*-hexadecane (bottom) and squalane (top) corresponding to the equilibrium 4-layer films (see Fig. 6). The confined film is the region between the solid lines. Note enhanced intramolecular and intermolecular order in the confined *n*-hexadecane film.

below about 5 layers, or $\leqslant 25$ Å) exhibits certain features characteristic to solid-like response; that is, when the confining gap width is slightly reduced [typically $\Delta D \sim 1-2$ Å), starting from one of the well-formed layered configurations of the film with n_L layers (corresponding to the maxima in the solvation force shown in Fig. 5(a)], the film ''yields'' through expulsion of approximately a layer-worth of molecular segments into the surrounding liquid, causing a sharp decrease in the confined film density. During further reduction of the gap width, the number of confined molecular segments remains almost constant [corresponding to the plateaus of n_{ncf} shown in Fig. 5(a)], with an associated increase of the confined film density [see n_{cfn}/D in Fig. 5(a)] which is accompanied by enhancement of the order in the layered structure of the film. This process continues until a gap width corresponding to a maximally ordered layered film (with $n_L - 1$ layers) is reached, for which the confined film density maximizes. This sequence of events repeats with a period of $\sim 4.5-5$ Å.

At this juncture we reemphasize that the states of the confined films which we analyze here are all at equilibrium conditions. Consequently, we argue that the different nature of the layering transitions in the *n*-hexadecane and squalane films, reflects differences in the equilibrium properties of the confined films of the two materials. In particular, we associate the aforementioned solid-like characteristics with a high degree of order in the layered *n*-hexadecane confined film, while the liquid-like nature found for the squalane case is correlated with frustration of the order in the confined film, caused mainly by branching.[44]

B. Structure and dynamics

As alluded to above, while organization of the confined film density into layered structures, with the number of layers dependent on the gap width, occurs for both the *n*-hexadecane and squalane films, the degree of order in the two films is different with that in the shorter linear alkane being higher. This may be ascertained from close inspection of the density profiles of the two systems shown in Figs. 2 and 3, where the minima between layers are deeper for *n*-hexadecane along with the occurrence, on each side of the squalane film, of small peaks between the density maxima corresponding to the layer closest to the solid interface and the second layer in, as well as from inspection of molecular configurations of the films, such as those shown for the equilibrated 4-layer films in Figs. 6 and 7. The side views of the films in Fig. 6 show enhanced layering order in the *n*-hexadecane film as compared to the squalane one, and the degree of in-plane intermolecular order in the first layer (interfacial layer closest to the solid surface) is clearly larger (see Fig. 7) in the linear alkane film (similarly for the second layer in, not shown). Indeed statistical analysis shows that for the 4-layer films the probabilities for one end of a molecule to be in the interfacial layer (designated as the first layer; note that by symmetry the interfacial layers on both sides of the film are equivalent, therefore we average our results for both interfaces) and the other end to be located either at the first, second, or third layer, are: $f_{ee}^{(1,i)}$(*n*-hexadecane) = 0.8, 0.12, and 0.08 for $i=1,2,3$, respectively, while for the squalane film these probabilities are almost evenly distributed, $f_{ee}^{(1,i)}$(squalane)= 0.33, 0.37, 0.30, indicating a high degree of interlayer interdigitation (bridging) in the longer branched alkane film. Additionally, for molecules with one end in one of the middle layers (desig-

Downloaded¬04¬Feb¬2004¬to¬130.207.165.29.¬Redistribution¬subject¬to¬AIP¬license¬or¬copyright,¬see¬http://jcp.aip.org/jcp/copyright.jsp

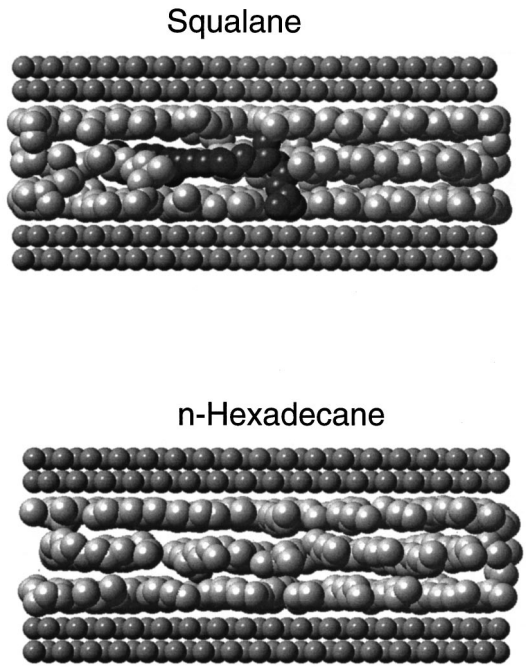

FIG. 8. Side views (in slices) through the *n*-hexadecane (bottom) and squalane (top) films, illustrating molecular interlayer interdigitation (dark shaded molecule) in the squalane film. The small spheres correspond to the surface layers of the gold substrates.

nated as layers 2 and 3) the probabilities that one end of the molecule is in one of these layers and the other is found either in the same layer or in the other one are: $f_{ee}^{(2,i)}$(*n*-hexadecane) = 0.6 and 0.4 for $i=2$ and 3, respectively, and $f_{ee}^{(2,i)}$(squalane) = 0.38 and 0.62, respectively, indicating a higher degree of interlayer interdigitation for molecules in the middle layers of the films, with a larger degree for the squalane film. A similar analysis but for the probabilities of one end of a molecule to be in the interfacial layer (layer 1 or 4) and the middle segment of the molecule to be located either in the same layer or in the middle layers of the film (layers 2 and 3) yields $f_{em}^{(1,i)}$(*n*-hexadecane) = 0.9, 0.08, and 0.02 for $i=$ 1, 2, and 3, respectively, and $f_{em}^{(1,i)}$(squalane) = 0.5, 0.39, 0.11, indicating that for the hexadecane film the small amount of interlayer interdigitation involves mainly the molecular tails, while for the squalane film a larger part of the molecule may be distributed between neighboring layers; the corresponding results for the middle layers of the films, $f_{em}^{(2,i)}(i=2,3)$, are: for *n*-hexadecane $f_{em}^{(2,2)}=0.79$, $f_{em}^{(2,3)}=0.21$, and for the squalane film $f_{em}^{(2,2)}=0.63$ and $f_{em}^{(2,3)}=0.37$. A similar analysis for the 3-layer *n*-hexadecane film gives: $f_{ee}^{(1,i)}$ = 0.9, 0.1 and $f_{em}^{(1,i)}$ = 0.94, 0.06 for $i=1,2$, respectively, and for the squalane film: $f_{ee}^{(1,i)}$ = 0.32, 0.55, and 0.13 for $i=1,2,3$, respectively (indicating that over 10% of the molecules bridge the two interfaces in the 3-layer squalane system), and $f_{em}^{(1,i)}$ = 0.65, 0.3, and 0.05. The selected molecular configurations displayed in Fig. 8 illustrate interlayer interdigitation in a 3-layer squalane film and no interdigitation in a corresponding *n*-hexadecane film.

The degree of order in the films can also be analyzed in terms of the order parameter $P_2(\cos\theta)=\langle(3\cos^2\theta-1)/2\rangle$, where θ is the angle formed between bond vectors connecting neighboring segments of the molecules and the direction normal to the surface, and the angular brackets denote averaging over all bonds in the regions (confined or bulk) and over the MD simulation. The results displayed in Fig. 9, show that in the bulk regions the molecular bonds do not exhibit any orientational order, i.e., $P_2(\cos\theta)\approx 0$. On the other hand in the confined films they show a tendency to lie preferentially parallel to the confining surfaces with the degree of that preferred orientation being larger in the *n*-hexadecane film. Furthermore, the degree of preferential orientational order [i.e., more negative values of $P_2(\cos\theta)$] oscillates as a function of the gap width, with local maximal orientational ordering achieved for gap widths corresponding to well-formed layers (i.e., solvation force maxima in Fig. 5), with intervening states of reduced orientational order corresponding to the transitions between layered states of the films as D is varied.

Finally, we show in Fig. 9 the torsional angle transition rates between *trans* and *gauche* conformations of the molecules. We observe that in the bulk region of *n*-hexadecane the transition rates are higher than in the bulk squalane liquid. The transition rates in the confined systems are lower than their corresponding bulk values, and exhibit an oscillatory behavior as a function of the gap width, with local minima of the transition rates occurring for values of D corresponding to well-formed layers. The amplitudes of the oscillations of the transition rates versus D are larger for the *n*-hexadecane film and they increase as the confining gap width is reduced.

These results correlate with those discussed above pertaining to structural properties, showing that both structural and dynamical characteristics of complex liquids are influenced greatly by their confinement. Moreover, our simulations revealed dependencies of the various degrees of order in the films (layering, in-plane order, and orientational ordering) on the complexity of the molecular constituents, and on the degree of confinement.

IV. SUMMARY

In this paper, equilibrium structures, solvation forces, and conformational dynamics of thin confined films of *n*-hexadecane and squalane were investigated using a new grand canonical ensemble molecular dynamics method for simulations of confined liquids. The method combines constant pressure simulations with a computational cell containing solid surfaces and both bulk and confined liquid regions in equilibrium with each other (Fig. 1), allowing investigations of confined films under conditions similar to those used in surface force apparatus and tip-based experiments.

Our studies provide insights into the nature of equilibrium confined liquids and the effects of molecular structure on the properties of such systems. For both the straight molecular chain liquid (*n*-hexadecane) and for the branched one (squalane) layered density oscillations in the confined films were found, with the number of layers depending on the

Downloaded¬04¬Feb¬2004¬to¬130.207.165.29.¬Redistribution¬subject¬to¬AIP¬license¬or¬copyright,¬see¬http://jcp.aip.org/jcp/copyright.jsp

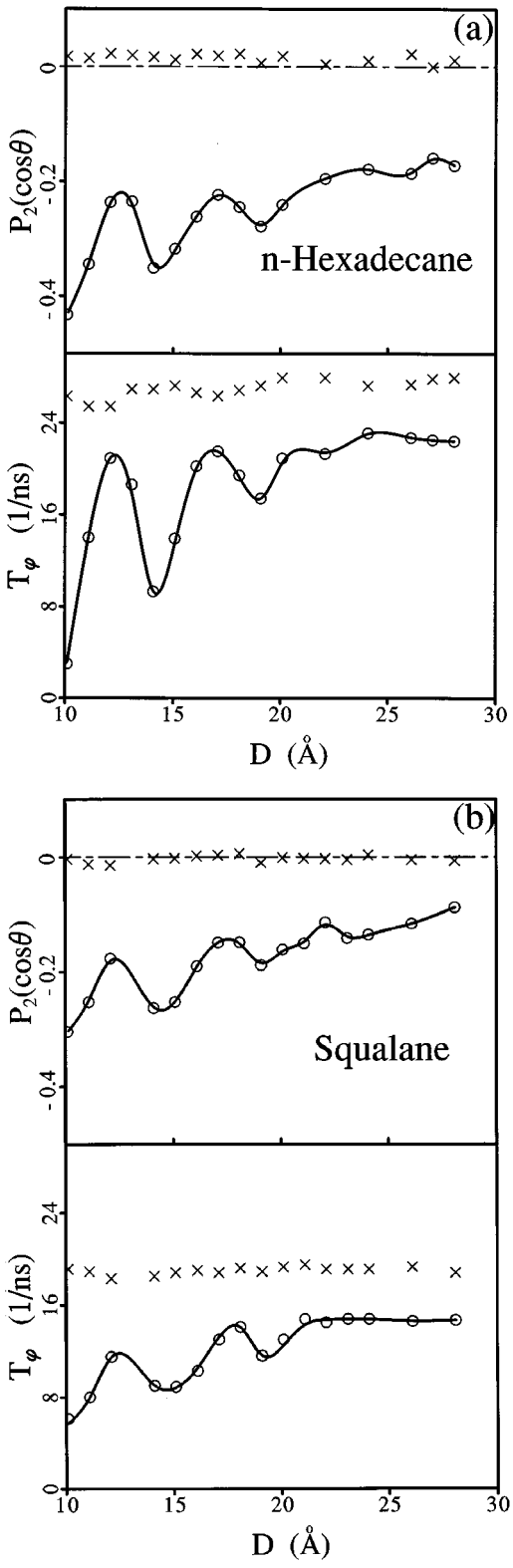

FIG. 9. Segment-bond order parameter, $P_2(\cos\theta)$, in the top panels, and *trans-gauche* (and vice versa) transition rates, T_ϕ (in units of 1/ns) in the bottom panels, plotted versus the gap width, D, in Å, for the equilibrium states of the *n*-hexadecane (a) and squalane (b) systems. The crosses correspond to values obtained for the bulk liquids outside the confinement, and the solid lines connect values calculated for the confined films.

width of the confinement. The *n*-hexadecane confined film exhibits enhanced layered order, as well as a higher degree of in-plane molecular ordering, compared to those found for the squalane film, with the latter showing a high tendency for interlayer molecular interdigitation (see Figs. 2, 3, 6–8). Reduced conformational (*trans-guache*) transition rates in the confined films, compared to their bulk values, are found, and their oscillatory dependence on the degree of confinement is analyzed, showing smaller transition rates for the well-formed layered states of the films (Fig. 9).

The solvation force oscillations as a function of the gap width for the straight chain, *n*-hexadecane, liquid are more pronounced exhibiting attractive and repulsive regions, while for the branched alkane the solvation forces are mostly repulsive, with the development of shallow local attractive regions for small values of the gap width (Fig. 4). These results correlate with recent observations using SFA measurement on confined films of squalane,[18,19] showing the influence of molecular structure (i.e., moderate degree of branching) on the character of the solvation forces. Furthermore, the nature of the transitions, and equilibrium intermediate states, between well-formed layered configurations is different in the two systems, with the *n*-hexadecane film exhibiting solid-like characteristics portrayed by step-like variations in the number of confined segments occurring in response to a small decrease (~1–2 Å) in the gap width, starting from well-layered states of the film [Fig. 5(a)]. On the other hand the behavior of the squalane film is liquid-like, exhibiting a monotonic continuous decrease in the number of confined segments as the gap width is decreased [Fig. 5(b)]. These characteristics, which are correlated with the above mentioned structural properties of the confined films, suggest that liquids with molecular structures which are more conducive to formation of ordered configurations (such as globular, or low-molecular weight straight chain molecules) would develop solid-like characteristics under confinement, while confined films made of more complex molecular structures (e.g., a moderate degree of branching, as in squalane), where ordering is frustrated due to the molecular structural complexity, would exhibit a higher tendency to behave in a liquid-like manner. In this context we remark that indeed solid-like behavior, under the sole effect of confinement (i.e., with no lateral relative shear motion between the confining surfaces) has been observed recently[19] in SFA experiments for semispherical molecules (OMCTS).

ACKNOWLEDGMENTS

This work is supported by the DOE, and the AFOSR. Computations were performed on CRAY Computers at the Pittsburgh Supercomputing Center and at the GIT Center for Computational Materials Science.

[1] For a recent review see, B. Bhushan, J. N. Israelachvili, and U. Landman, Nature **374**, 607 (1995).
[2] *Fundamentals of Friction: Macroscopic and Microscopic Processes*, edited by I. L. Singer and H. M. Pollock (Kluwer, Dordrecht, 1992).
[3] *Physics of Sliding Friction*, edited by B. N. J. Persson and E. Tosatti (Kluwer, Dordrecht, 1996).

Downloaded¬04¬Feb¬2004¬to¬130.207.165.29.¬Redistribution¬subject¬to¬AIP¬license¬or¬copyright,¬see¬http://jcp.aip.org/jcp/copyright.jsp

[4] *Handbook of Micro/Nano Tribology*, edited by B. Bhushan (CRC, Boca Raton, Florida, 1995).
[5] See articles in Langmuir **12**, 4481–4609 (1996).
[6] See U. Landman, W. D. Luedtke, and E. M. Ringer in Ref. 2, p. 463.
[7] U. Landman, W. D. Luedtke, and J. Gao, Langmuir **12**, 4514 (1996).
[8] M. Robbins and E. D. Smith, Langmuir **12**, 4543 (1996).
[9] M. D. Perry and J. A. Harrison, Langmuir **12**, 4552 (1996).
[10] H. T. Davis, *Statistical Mechanics of Phases, Interfaces and Thin Films* (VCH, New York, 1996).
[11] J. N. Israelachvili, *Intermolecular and Surface Forces*, 2nd ed. (Academic, New York, 1992).
[12] B. N. J. Persson, *Sliding Friction* (Springer, Berlin, 1997).
[13] P. B. Babuena, D. Berry, and K. E. Gubbins, J. Phys. Chem. **97**, 937 (1993).
[14] K. Walley, K. S. Schweizer, J. Peanasky, L. Cai, and S. Granick, J. Phys. Chem. **100**, 3361 (1994).
[15] M. Urbakh, L. Daikhin, and J. Klafter, J. Chem. Phys. **103**, 10 707 (1995); M. G. Rozman, M. Urbakh, and J. Klafter, Phys. Rev. Lett. **77**, 683 (1996).
[16] (a) C. L. Rhykerd, Jr., M. S. Schoen, D. Diester, and J. Cushman, Nature **330**, 461 (1987), see citations 38–41 cited in Ref. 1; (b) U. Landman, W. D. Luedtke, and M. W. Ribarsky, J. Vac. Sci. Technol. A **7**, 2829 (1989).
[17] J. N. Israelachvili and R. G. Horn, J. Chem. Phys. **35**, 1400 (1981).
[18] S. Granick, A. L. Demirel, L. L. Cai, and J. Peanasky, Isr. J. Chem. **35**, 75 (1995).
[19] J. Klein and E. Kumacheva, Science **269**, 816 (1995).
[20] H. K. Christenson, D. W. R. Gruen, R. G. Horn, and J. N. Israelachvili, J. Chem. Phys. **87**, 1834 (1987).
[21] M. W. Ribarsky and U. Landman, J. Chem. Phys. **97**, 1937 (1992), and references therein.
[22] (a) U. Landman, W. D. Luedtke, J. Ouyang, and T. K. Xia, Jpn. J. Appl. Phys. **32**, 1444 (1993); (b) W. D. Luedtke and U. Landman, Comput. Mater. Sci. **1**, 1 (1992).
[23] U. Landman and W. D. Luedtke, MRS Bull. **17**, 36 (1993).
[24] S. Gupta, D. C. Koopman, G. B. Westerman-Clark, and I. A. Bitsanis, J. Chem. Phys. **100**, 8444 (1994).
[25] E. Manias, G. Hadziioannou, and G. ten Brinke, Langmuir **12**, 4587 (1996).
[26] J. N. Israelachvili, S. J. Kott, M. Gee, and T. A. Witten, Macromolecules **22**, 4247 (1989).
[27] M. L. Gee and J. N. Israelachvili, J. Chem. Soc. Faraday Trans. (2) **86**, 4049 (1990).
[28] For simulations of confined alkanes with a single pendant methyl, where force oscillations similar to those found for the corresponding straight chain alkanes, see: (a) Y. Yang, K. Hill, and J. G. Harris, J. Chem. Phys. **100**, 3276 (1994); (b) J. Ouyang, Ph.D. dissertation, Georgia Institute of Technology, 1995; J. Ouyang, W. D. Luedtke, and U. Landman, Bull. Am. Phys. Soc. **40**, 425 (1995).
[29] J. N. Israelachvili (private communication).
[30] S. Granick, Science **253**, 1374 (1991).
[31] D. Y. C. Chan and R. G. Horn, J. Chem. Phys. **83**, 5311 (1985).
[32] J. N. Israelachvili, J. Colloid. Interface Sci. **110**, 263 (1986).
[33] G. Reiter, A. L. Demirel, and S. Granick, Science **263**, 1741 (1994).
[34] H. Yoshizawa, P. McGuiggan, and J. N. Israelachvili, Science **259**, 1305 (1993).
[35] P. A. Thompson and M. O. Robbins, Science **250**, 792 (1990); M. O. Robbins and P. A. Thompson, *ibid.* **253**, 916 (1991).
[36] B. N. J. Persson, Phys. Rev. B **50**, 4771 (1994).
[37] J. Gao, W. D. Luedtke, and U. Landman, Science **270**, 605 (1995).
[38] J, van Alsten and S. Granick, Macromolecules **23**, 4856 (1990); S. Granick and H.-W. Hu, Langmuir **10**, 3857 (1994); J. Peanasky, L. Cai, C. R. Kessel, and S. Granick, *ibid.* **10**, 3874 (1994).
[39] I. K. Snook and W. J. van Megen, J. Chem. Phys. **72**, 2907 (1980).
[40] W. J. van Megen and I. K. Snook, J. Chem. Phys. **74**, 1409 (1981).
[41] M. Parrinello and A. Rahman, J. Appl. Phys. **52**, 7182 (1981). In deriving the equations of motion within the Parrinello-Rahman formalism, we take as our Lagrangian dynamical variables the scaled-space coordinates of the fluid particles and the component of the calculation cell along the x direction.
[42] M. Mondello and G. S. Grest, J. Chem. Phys. **103**, 7156 (1995).
[43] T. K. Xia, J. Ouyang, M. W. Ribarsky, and U. Landman, Phys. Rev. Lett. **69**, 1967 (1992).
[44] Similar simulations which we performed for simple spherical LJ fluids have shown an even more pronounced step-like behavior than that found by us for n-hexadecane [see Fig. 5(a)]. This indicates that solid-like behavior is enhanced in sufficiently thin confined liquids which pack well and exhibit a high degree of ordering, as in OMCTS (Ref. 19). Furthermore, recent simulations for n-tetracosane (n-$C_{24}H_{50}$) show a similar behaviour to that of n-hexadecane, leading us to conclude that the different behaviour of squalane is caused by branching rather than by increased chain-length; J. Gao, W. D. Luedtke, and U. Landman (in preparation).

Downloaded¬04¬Feb¬2004¬to¬130.207.165.29.¬Redistribution¬subject¬to¬AIP¬license¬or¬copyright,¬see¬http://jcp.aip.org/jcp/copyright.jsp